Plant, Cell & Environment

Plant, Cell and Environment (2014) **37**, 2738–2753 doi: 10.1111/pce.12353

Original Article

Physiological characterization and genetic modifiers of aberrant root thigmomorphogenesis in mutants of *Arabidopsis thaliana MILDEW LOCUS O* genes

Przemyslaw Bidzinski[1]*, Sandra Noir[1†], Shermineh Shahi[1‡], Anja Reinstädler[1,2], Dominika Marta Gratkowska[1§] & Ralph Panstruga[1,2]

[1]*Department of Plant-Microbe Interactions, Max-Planck-Institute for Plant Breeding Research, 50829 Cologne, Germany and*
[2]*Institute for Biology I, Unit of Plant Molecular Cell Biology, RWTH Aachen University, 52056 Aachen, Germany*

ABSTRACT

Root architecture and growth patterns are plant features that are still poorly understood. When grown under *in vitro* conditions, seedlings with mutations in *Arabidopsis thaliana* genes *MLO4* or *MLO11* exhibit aberrant root growth patterns upon contact with hard surfaces, exemplified as tight root spirals. We used a set of physiological assays and genetic tools to characterize this thigmomorphogenic defect in detail. We observed that the *mlo4*/*mlo11*-associated root curling phenotype is not recapitulated in a set of mutants with altered root growth patterns or architecture. We further found that *mlo4*/*mlo11*-conditioned root curling is not dependent upon light and endogenous flavonoids, but is pH-sensitive and affected by exogenous calcium levels. Based upon the latter two characteristics, *mlo4*-associated root coiling appears to be mechanistically different from the natural strong root curvature of the Arabidopsis ecotype Landsberg *erecta*. Gravistimulation reversibly overrides the aberrant thigmomorphogenesis of *mlo4* seedlings. Mutants with dominant negative defects in α-tubulin modulate the extent and directionality of *mlo4*/*mlo11*-conditioned root coils, whereas mutants defective in polar auxin transport (*axr4*, *aux1*) or gravitropism (*pgm1*) completely suppress the *mlo4* root curling phenotype. Our data implicate a joint contribution of calcium signalling, pH regulation, microtubular function, polar auxin transport and gravitropism in root thigmomorphogenesis.

Key-words: calcium; gravitropism; MLO; pH regulation; polar auxin transport; tubulin function.

Correspondence: R. Panstruga. Fax: +49 241 80 22637; e-mail: panstruga@bio1.rwth-aachen.de

*Present address: INRA – UMR BGPI, Campus International de Baillarguet, CIRAD TA A-54/K, 34398 Montpellier Cedex, France.
†Present address: Institut de Biologie Moléculaire des Plantes – CNRS, 12 rue Général Zimmer, 67084 Strasbourg, France.
‡Present address: Plant Pathology, Swammerdam Institute for Life Sciences, Faculty of Science, University of Amsterdam, PO Box 94215, 1090 GE Amsterdam, The Netherlands.
§Present address: Department of Protein Biosynthesis, Institute of Biochemistry and Biophysics, Polish Academy of Sciences, Pawińskiego 5a, 02-106 Warszawa, Poland.

INTRODUCTION

Plants are immobile and have to actively adapt to the encountered environment. They are anchored with roots, which are indispensable organs for nutrient and water uptake. Root growth is a very flexible trait that has to adjust to the existing conditions and is also being used as a model to study developmental plasticity (Malamy 2005). Although plasticity of root development is well documented, it is still poorly understood at the level of molecular mechanisms.

Directional root expansion requires the interpretation and integration of various environmental stimuli, including gravity, the availability of water and nutrients, and the presence of physical barriers. Plant roots react with alterations in growth directionality (tropisms) and modification of growth patterns (morphogenic adaptations) to these signals, of which thigmotropism and thigmomorphogenesis (the change of growth direction and growth patterns in response to a mechanical stimulus; Migliaccio & Piconese 2001; Jaffe *et al*. 2002; Chehab *et al*. 2009) are arguably one of the least studied. Although the actual touch sensors remain obscure (Telewski 2006), it is known that plant responses to physical stimulation include calcium (Ca^{2+}) signalling (Braam & Davis 1990; Monshausen *et al*. 2009), the generation of reactive oxygen species and changes in the extracellular and cytoplasmic pH (Monshausen *et al*. 2009), and the activation of dedicated transcriptional programmes (Kimbrough *et al*. 2004; reviewed in Chehab *et al*. 2009). It seems that most of the directional root growth activities, including thigmoresponses, are modulated by hormone homeostasis and especially by distribution patterns of the phytohormone auxin (Osmont *et al*. 2007). In addition, a contribution of the gaseous phytohormone ethylene in the regulation of touch responses in Arabidopsis is controversially discussed (Johnson *et al*. 1998; Anten *et al*. 2006; Yamamoto *et al*. 2008). Recently, it was found that jasmonic acid, another phytohormone, which is primarily known for its role in plant responses to biotic and abiotic stresses, is required for thigmomorphogenic responses in *Arabidopsis thaliana* (Chehab *et al*. 2012).

To date, few Arabidopsis mutants with defects in touch-related alterations in root growth patterns have been identified. One of these is *mca1*, which has a defect in mechanosensing (Nakagawa *et al*. 2007). Roots of *mca1* (or

mca1 mca2) seedlings are unable to penetrate the boundary layer of a two-phase agar system. MCA1 and MCA2 are sequence-related to the yeast mechanosensitive Ca^{2+} channel component Mid1 and have been implicated in Ca^{2+} uptake in Arabidopsis roots (Nakagawa *et al*. 2007; Yamanaka *et al*. 2010). Other genes with a documented role in thigmomorphogenesis are *MLO4* (At1g11000) and *MLO11* (At5g53760), two members of the *MLO* family encoding plant-specific integral membrane proteins with a serpentine heptahelical topology (Devoto *et al*. 1999, 2003; Chen *et al*. 2009). Members of this protein family are best known for their role in the modulation of the powdery mildew disease (Panstruga 2005; Bai *et al*. 2008; Humphry *et al*. 2011). However, other family members play a role in plant developmental processes (Chen *et al*. 2009; Kessler *et al*. 2010). When grown *in vitro* on minimal medium, *mlo4* and *mlo11* mutant seedlings exhibit spiral-like root growth patterns upon contact with a physical barrier (Supporting Information Movies S1–S3). Results from pharmacological, genetic and cell biological experiments implicated auxin distribution patterns and possibly flavonoids, which can act as endogenous auxin transport regulators, in the control of this phenotype (Chen *et al*. 2009). Mutations in a third member of the same phylogenetic clade, *MLO14* (At1g26700), do not result in any obvious phenotype (Chen *et al*. 2009).

Several lines of evidence link MLO function with Ca^{2+} signalling. Firstly, MLO proteins harbour a functional binding domain for the ubiquitous Ca^{2+} sensor, calmodulin, in their C-terminal cytoplasmic region (Kim *et al*. 2002; Devoto *et al*. 2003; Kim & Hwang 2012). Binding of calmodulin to this domain increases during the entry phase of the barley powdery mildew pathogen (Bhat *et al*. 2005). Secondly, successful host cell entry into barley epidermal cells by powdery mildew sporelings is promoted by the exogenous application of Ca^{2+} and suppressed by the addition of calmodulin inhibitors (Kobayashi *et al*. 2007). Thirdly, the powdery mildew-resistant phenotype of barley *mlo* mutants can be partially suppressed by the exogenous application of Ca^{2+} (Bayles & Aist 1987). Fourthly, some constitutive active and dominant negative variants of calcium-dependent protein kinases (CDPKs) partially compromise otherwise highly efficient *mlo* resistance in barley (Freymark *et al*. 2007). In summary, these data suggest a functional link between Ca^{2+} signalling and MLO activity. Nevertheless, the molecular details of this interconnection are still unknown.

Here, we provide a thorough characterization of the aberrant root morphogenesis phenotype found in Arabidopsis *mlo4* and *mlo11* mutants. We used a set of physiological assays and genetic tools to unravel requirements of this phenotype. Our data implicate a joint contribution of Ca^{2+} signalling, pH regulation, microtubular function, polar auxin transport and gravitropism in root thigmomorphogenesis.

MATERIALS AND METHODS

Plant materials

All plant materials used in this study are described in Supporting Information Methods S1.

Plant growth conditions

Plants were cultivated as previously described by Chen *et al*. (2009), unless differentially stated. Briefly, ethanol-sterilized seeds were air-dried and then distributed *via* toothpicks on plates with minimal medium in regular distance to keep homogenous growth conditions. The minimal medium was buffered with 0.05% 2-(N-morpholino)ethanesulfonic acid MES, supplemented with 0.25% sucrose, pH adjusted to 5.7 and solidified with 0.5% (w/v) bactoagar (Research Products International, Mt. Prospect, IL, USA). For some experiments, where indicated, we used Murashige and Skoog medium [MS, 0.9% (w/v) phytoagar and 1% (w/v) sucrose, pH adjusted to 5.8 with NaOH]. Samples for comparisons were placed on the same plate to minimize variations owing to exogenous factors. Plates were incubated at 4 °C for 48–72 h and then transferred to growth cabinets set at 21 °C and equipped with a top fluorescent light source yielding 140 μmol m^{-2} s^{-1}. Most of the experiments were performed in a 16 h/8 h light/dark cycle, and some experiments were performed in darkness or constant light as indicated. Results were typically recorded at 7 d after being transferred to the growth cabinet, unless indicated otherwise.

Physiological assays and root span measurements

Seeds were treated as described earlier. To correct for growth variation, seedlings were grown on at least three plates along with the controls, and each experiment was repeated at least twice. Any other modifications to the minimal medium are indicated at the corresponding experiment. Root curling was measured as described (Chen *et al*. 2009), with minor modifications. The width of the plates was verified with a ruler and then used to set a scale in the ImageJ image analysis software used for measurements of root span (http://rsb.info.nih.gov/ij/). Root span was assessed by measuring the distance from the root tip to the root base on the photographs. Statistical analysis was performed with Student's *t*-test (two-tailed, equal variance). All pictures, except the ones shown in Fig. 1, which were taken from above, were taken from the bottom of the plate. In some cases, the final image is a collage of several pictures.

Root gravitropism assay

After stratification and sterilization, seedlings were grown vertically on MS medium for 8 d in a 12 h light/dark regime. Plates were then placed in dark conditions and root curvatures of the seedlings were measured every 2 h for 12 h after gravistimulation (90° re-orientation with respect to the gravity vector).

Combined root touch and gravity response

Seeds were treated as described earlier. After 2–3 d of stratification, plates were placed horizontally in the growth chamber with top light fluorescent bulbs. Four days later,

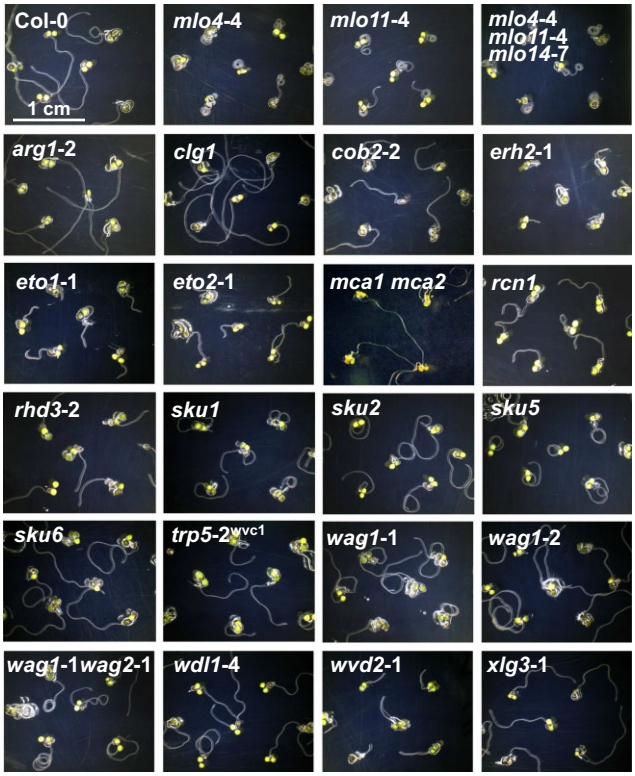

Figure 1. Phenotypes of mutants with aberrant root growth patterns grown on minimal medium do not resemble *mlo4*-like root curling. Seedlings of the indicated genotypes were grown on horizontal plates with minimal medium. Quantification of *mlo4*-like root curling and details of tested mutants are given in Supporting Information Table S1. Images of additional alleles are presented in Supporting Information Fig. S2. Quantification of the root span is provided in Supporting Information Fig. S1. Each line was tested in at least three independent, randomized experiments.

plates were turned vertically and some plates were wrapped in aluminium foil to eliminate the effect of negative phototropism. Two days later, plates were placed back to the original horizontal position and pictures were taken 2 d later.

Combined root touch and gravitropism assay with an embedded barrier

Seeds were treated as described earlier. On the first layer of 50 mL of minimal medium, a sterile nylon mesh or a microscopic coverslip was placed and a second layer of 50 mL of minimal medium was poured on top. After 2–3 d of stratification, plates were placed horizontally in the growth chamber with the top facing the lights. The phenotype was assessed and pictures were taken from 4 to 7 d thereafter.

Hypocotyl gravitropism assay

After stratification and sterilization, seedlings were grown vertically on MS medium for 3 d in the dark prior to gravistimulation (90° re-orientation with respect to the gravity vector). Hypocotyl curvature was judged qualitatively 12 h later.

Shoot gravitropism assay

Plants were grown in soil until the early bolting stage and then pots were transferred to dark conditions and turned by 90° for gravistimulation. Shoot curvature was judged qualitatively 3 h later.

Auxin sensitivity assay

After stratification and sterilization, seedlings were grown vertically on the MS medium in a 12 h light/dark cycle. Five-day-old seedlings were transferred on the MS medium supplemented with the synthetic auxin 2,4-dichlorophenoxyacetic acid (2,4-D; Sigma-Aldrich, Munich, Germany). Root length elongation was measured 3 d later.

Lugol staining

Seedlings were grown on minimal medium for 7 d, as described earlier. Seedlings were transferred to Lugol solution (I_2/KI; Sigma-Aldrich) and incubated for 5 min. Then, seedlings were briefly washed with water, mounted on a slide with chloral hydrate (Sigma-Aldrich) and observed immediately. Observations and images were taken with Nomarski interference optics using a ZEISS Axio Imager.A2 microscope (Carl Zeiss, Jena, Germany) and AxioVision software (Carl Zeiss).

DPBA staining

For visualization of flavonoid accumulation, root tips of 5-day-old seedlings grown on MS medium were stained for a few minutes in 0.25% diphenylboric acid 2-amino ethyl ester (DPBA)/0.005% Triton X-100 (Sigma-Aldrich). DPBA complexes with flavonoids and greatly enhances their fluorescent properties (Buer *et al.* 2010). Fluorescence was imaged with an LSM510 confocal microscope (Carl Zeiss) using a 488 nm argon laser line and a 505–550 nm bandpass filter.

Suppressor mutant screening

Seeds (~10k) of the *MLO4* (At1g11000) *Arabidopsis* T-DNA insertion line *mlo4*-3 (GABI-KAT_023A10; Col-0 background) were mutagenized by treatment with ethyl methane sulfonate (EMS, Sigma-Aldrich). The EMS-treated M_1 seeds were washed 15 times with water and sown. Bulks of M_2 seeds from 25 mutagenized plants were collected. Screening for suppressor mutants (loss of the root curling phenotype) was performed on the basis of 300–500 seeds per M_2 bulk on minimal medium and scored at 7 d after sowing. Candidate mutants were confirmed in the M_3 generation.

Mapping and cloning

mlo4-3 suppressor candidates (Col-0 background) were crossed to *mlo4*-1 mutant (Ws-0 background) to generate an F_2 mapping population. A set of SSLP markers polymorphic between Col-0 and Ws-0 (Supporting Information Table S2)

was selected to perform PCR-based first-pass mapping. Further markers and sequencing of candidate genes were used for fine mapping.

DNA sequencing

DNA sequences were determined at Max Planck Genome Centre Cologne, Germany, on Applied Biosystems (Weiterstadt, Germany) Abi Prism 377, 3100 and 3730 sequencers using BigDye-terminator v3.1 chemistry. Premixed reagents were from Applied Biosystems (Carlsbad, CA, USA).

RESULTS

Known mutants affected in root growth pattern or architecture do not show *mlo4*-like defects in root thigmomorphogenesis

We aimed to analyse whether the aberrant root thigmomorphogenesis of *mlo4* and *mlo11* mutants might also be attributed to other known mutants affected in root development and/or architecture. Phenocopies of the *mlo4*/*mlo11* root growth pattern might point to the involvement of the respective gene(s) in the same genetic pathway(s) as *MLO4* and/or *MLO11*. The comprehensive set of tested mutants comprised, among others, representatives with reported defects in root waving (e.g. *wag1*, *wag2*, *wvd2*, *xlg3*) and skewing (e.g. *sku1*, *sku2*, *sku5*, *sku6*) as well as the *mca1 mca2* double mutant, which has a defect in mechanoperception in roots (Supporting Information Table S1). While in our previous work (Chen *et al*. 2009) root span was a suitable parameter to discriminate between curling *mlo4*/*mlo11* and non-curling wild-type roots, it turned out to be a less appropriate parameter when mutants are affected in root elongation (Supporting Information Fig. S1). Therefore, we additionally scored the mutants subjectively for their phenotypic similarity in root growth to *mlo4*/*mlo11* (Supporting Information Table S1). The mutants tested showed a wide range of root growth patterns, but none clearly resembled the root thigmomorphogenesis phenotype of *mlo4* and *mlo11* mutants (Fig. 1 and Supporting Information Fig. S2). We observed the most severe phenotypes, disabling clear conclusions owing to seriously stunted roots, in the case of *erh2*-1, *eto1*-1, *eto2*-1 and *wvd2*-1. These mutants therefore were additionally grown up to 14 d, which nevertheless did not result in any further root elongation under our conditions. Notably, several seedlings of *wag1 wag2* double mutants, but not those of *wag1* or *wag2* single mutants, had root growth patterns that were, to some extent, similar to *mlo4* coils (Fig. 1 and Supporting Information Fig. S2). However, these spirals were never as tight as those observed in *mlo4*, and the penetrance of the phenotype was considerably lower than in the case of *mlo4* (98% curling for *mlo4*-4 roots versus 9% for *wag1*-1 *wag2*-1 and 36% for *wag1*-2 *wag2*-1 roots; Supporting Information Table S1). The *mca1 mca2* double mutant, which exhibits a defect in touch sensing, showed unaltered root growth. In summary, the *mlo4*/*mlo11*-like root curling phenotype does not clearly match the root growth pattern of any of the tested mutants.

mlo4 and *mlo11* root curling in darkness revisited

The dependence of the *mlo4* and *mlo11* phenotype on the presence/absence of light, the light intensity, the availability of nutrients and the presence of various small molecules was previously assessed (Chen *et al*. 2009). For most of these experiments, seedling and root phenotypes were followed up for up to 5 d after sowing. In the case of dark-grown seedlings, the major energy sink is the elongating hypocotyl, whereas root expansion is largely suppressed in this condition (Leyser & Day 2003). Therefore, the roots of 5-day-old plants grown on minimal medium in darkness are typically not well developed (see Fig. 4d,e in Chen *et al*. 2009), which may mask a potential root curling phenotype. Consequently, we now followed up the root phenotype in 7- to 14-day-old seedlings and observed that under these conditions, *mlo4*, *mlo11* and *mlo4 mlo11 mlo14* mutant seedlings developed their typical root spirals that were clearly distinct from the root curvature of Col-0 wild-type control seedlings (Fig. 2). These findings indicate that, contrary to previous belief (Chen *et al*. 2009), the root thigmomorphogenesis phenotype of these mutants is not light-dependent.

Aberrant *mlo4*- or *mlo11*-associated root thigmomorphogenesis does not depend upon flavonoid biosynthesis

We previously found that the exogenous application of some flavonoids suppresses *mlo4*-conditioned root curling (Chen *et al*. 2009). Given the known role of flavonoids in the regulation of polar auxin transport (Stenlid 1976; Santelia *et al*. 2008) and the dependence of aberrant *mlo4*-associated root thigmomorphogenesis on auxin distribution (Chen *et al*. 2009), this finding implicates a potential role for flavonoid accumulation patterns in the establishment of root curvature. To test this possibility on the basis of genetic means, we used a *tt4* T-DNA mutant. *TRANSPARENT TESTA4* (*TT4*) encodes chalcone synthase (CHS), which catalyses the entry step into the flavonoid biosynthetic pathway. Consequently, *tt4* null mutants lack any detectable flavonoid accumulation (Lepiniec *et al*. 2006). On minimal medium, both *mlo4 tt4* and *mlo11 tt4* double mutant seedlings formed root spirals that were indistinguishable from the root growth pattern of *mlo4* and *mlo11* single mutants, whereas root growth of the *tt4* single mutant was similar to that of Col-0 wild-type seedlings (Fig. 3a). In addition, we found seemingly unaltered gross flavonoid accumulation and tissue distribution patterns in *mlo4* and *mlo11* mutant roots (Fig. 3b). Since absence of endogenous flavonoids neither suppresses *mlo4* root curling nor induces unusual root curvature in *tt4* single mutants, flavonoid levels seem to have either little or no effect on the formation of *mlo4* root spirals.

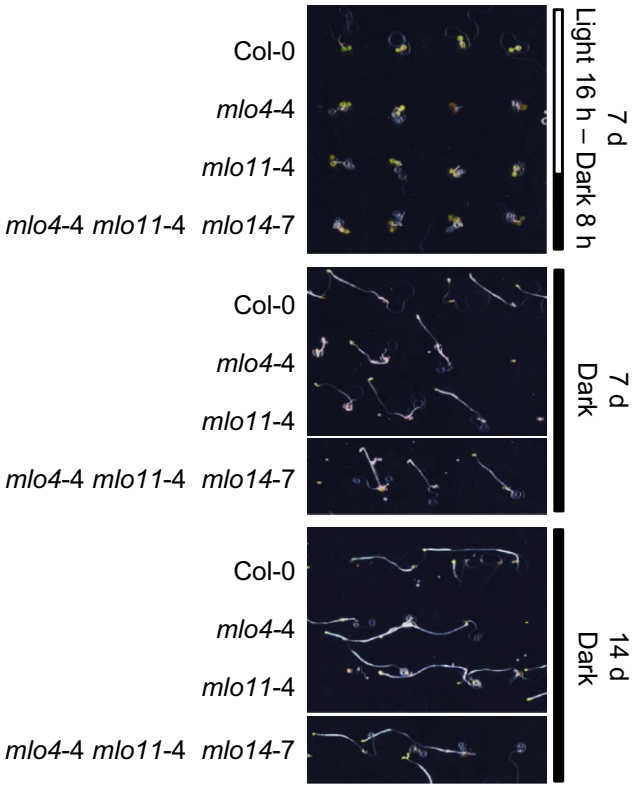

Figure 2. Root curling phenotypes of *mlo4* and *mlo11* mutants are light-independent. Seedlings of the indicated genotypes were either grown in standard conditions (16 h light/8 h dark; top panel), for 7 d in darkness (middle panel; minimal medium, 0.25% sucrose) or 14 d in darkness (bottom panel; minimal medium, 3% sucrose). In the latter two cases, after initial 6 h irradiation with white light (140 μmol m^{-2} s^{-1}), plates were wrapped in three layers of thick aluminium foil and kept on a side of the control plates. The seedlings were viable at the end of the experiment, and fully developed after transfer to soil. The different sucrose concentrations used represent the standard concentration (0.25%) and an elevated concentration (3%) to enable sufficient plant development in the prolonged absence of light. We previously showed that the sucrose concentration does not affect *mlo4*-conditioned root curling (Chen *et al*. 2009).

mlo4-conditioned root curling requires a mildly acidic environment

We next analysed the impact of the pH in the medium on the *mlo4*-conditioned root curling phenotype. We were able to test growth phenotypes in the pH range from ≈pH 4.5 to ≈pH 10.5 (medium pH adjusted with HCl or NaOH). At pH values below 3, the bactoagar did not solidify, even at 5% agar concentration, whereas pH values above 11 severely affected seed germination and seedling development. We included BCP (5′,5′-dibromo-ocresolsulfophthalein; bromocresol purple; pH range 5.2–6.8, visual colour transition: yellow to purple), as a colorimetric indicator of pH changes to the medium. Addition of BCP did not affect seedling development, since the same phenotypes were observed in the presence or absence of BCP. We noticed local medium acidification during seedling development, which was visible as yellowish patches on purple background in the zones of seedling growth on the plates with a pH above 6.5 (Fig. 4). The *mlo4*, *mlo11* and *mlo4 mlo11 mlo14* mutants developed the characteristic root curling phenotype at pH 4.6 and 5.6. On plates with pH 6.5, some mutant seedlings still formed root curls or roots were slightly wavy, which was a feature distinct from Col-0 wild-type plants. At higher pH (i.e. 8.8 and 10.4), mutant seedlings were indistinguishable from Col-0 wild-type seedlings (Fig. 4). The pH affected the root growth pattern of *mlo4*, *mlo11* and *mlo4 mlo11 mlo14* mutants in a similar manner. In summary, the data indicate that the formation of thigmomorphogenic root spirals in *mlo4*, *mlo11* and *mlo4 mlo11 mlo14* mutants is a pH-dependent phenomenon that requires mildly acidic medium conditions.

Exogenous application of Ca^{2+} suppresses the root curling phenotype of *mlo4* and *mlo11* mutants

As outlined in detail in the Introduction, several lines of evidence link MLO function to Ca^{2+} responses (Bayles & Aist 1987; Kim *et al*. 2002; Kobayashi *et al*. 2007). We therefore wondered whether exogenous application of Ca^{2+} may affect *mlo4*/*mlo11*-conditioned root curling. To test this possibility, seedlings were grown for 7 d on minimal medium

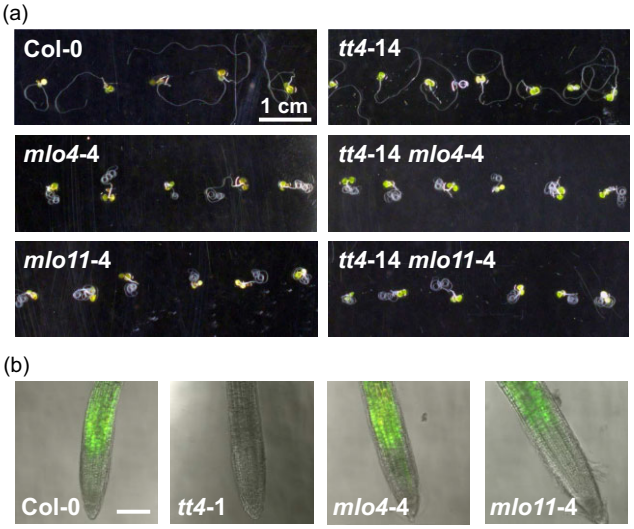

Figure 3. Flavonoids are dispensable for the root curling phenotype of *mlo4* and *mlo11* mutants. (a) Pictures of control and representative double mutant plants grown on minimal medium for 7 d on horizontal plates. Three lines for each double mutant combination were tested in two independent experiments. The same phenotype was observed in F_3 progeny of F_2 homozygous lines presented on the pictures. (b) Micrographs of diphenylboric acid 2-amino ethyl ester (DPBA) staining in root tips of indicated genotypes. Five-day-old seedlings grown on Murashige and Skoog (MS) medium were stained with DPBA and analysed by confocal laser scanning microscopy. Fluorescence is pseudo-coloured in green, overlaid on respective bright-field images. The micrographs are representative of two independent experiments. Scale bar: 100 μm.

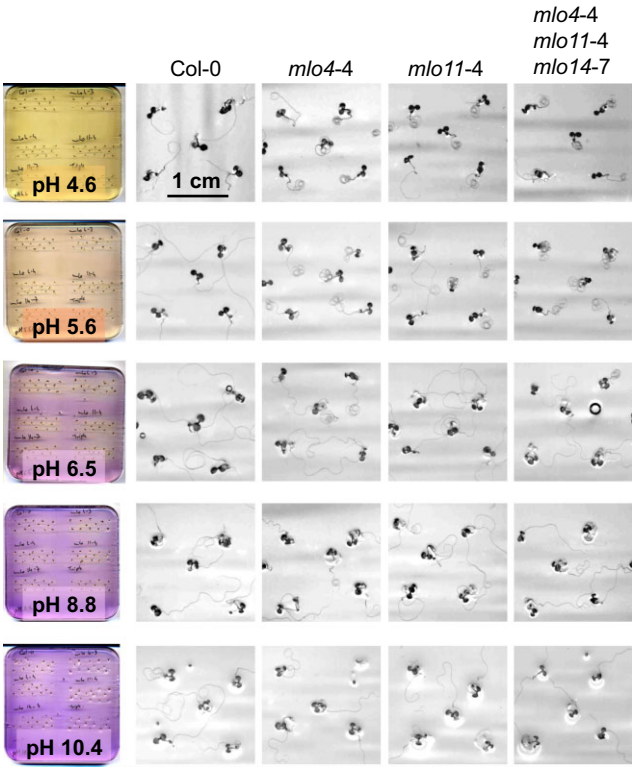

Figure 4. The root curling phenotype of *mlo4* and *mlo11* mutants depends upon the medium pH. Seedlings of the indicated genotypes were grown for 7 d on minimal medium with the pH adjusted to the values indicated in the left column. Example plates in that column were additionally supplemented with 0.04% (w/v) BCP (5′,5′-dibromo-ocresolsulfophthalein) to monitor pH changes during seedling development. Representative seedlings of the genotypes indicated are presented as close-ups in columns with the respective pH value of the minimal media. The same phenotypes were observed on the minimal medium with and without BCP. The experiment was repeated three times with similar results.

supplemented with various concentrations of either $CaCl_2$ (Fig. 5a) or other salts as controls (Fig. 5b and Supporting Information Fig. S3). Addition of 1 mM $CaCl_2$ significantly increased the root span of the *mlo11*, but not the root span of the *mlo4* or *mlo4 mlo11 mlo14* mutant (Fig. 5b). At 2.5 mM $CaCl_2$, the root span of the *mlo11* mutant was indistinguishable from Col-0 control plants, and the root curling phenotype was fully suppressed. In the case of the *mlo4* and *mlo4 mlo11 mlo14* mutants, suppression of root curling required 5–10 mM $CaCl_2$, and even at these concentrations, the effect was incomplete. A further increase up to 20 mM $CaCl_2$ revealed some inhibitory effects on the root span of Col-0 and *mlo11* seedlings, possibly because of toxicity (Fig. 5b).

To assess the Ca^{2+} specificity of these effects, we tested additional salts with similar chemical characteristics (neighbouring Ca^{2+} in the Periodic Table of Elements) for their impact on thigmotropic root curling. Addition of KCl did not affect the root curling phenotype, whereas $SrCl_2$ behaved similarly as $CaCl_2$ and fully (at 1 mM, *mlo11*) or partially (at 2.5–5 mM, *mlo4* and *mlo4 mlo11 mlo14*) suppressed root curling and had an inhibitory effect on root growth at higher concentrations (10–20 mM; Supporting Information Fig. S3a). The ability of $SrCl_2$ to suppress root curling is not surprising in the light of other experimental evidence that at least some biological functions of Ca^{2+} might be replaced by Sr^{2+} (Miledi

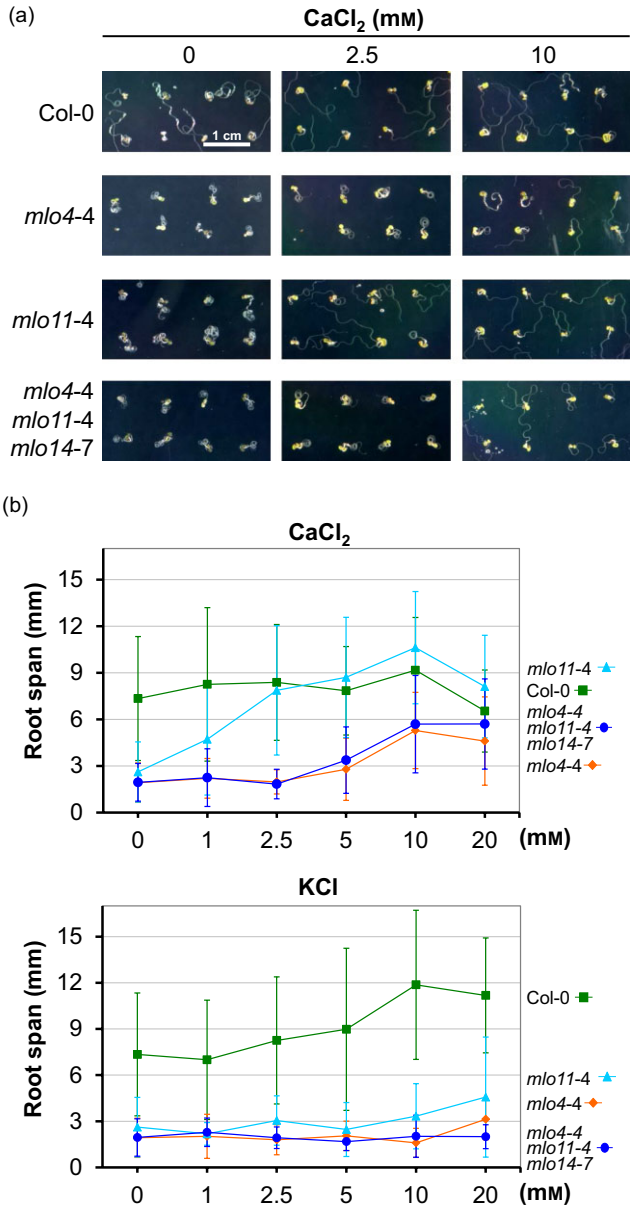

Figure 5. Exogenous application of calcium chloride suppresses the root curling phenotype of *mlo4* and *mlo11* mutants. (a) Representation of the phenotypes of indicated genotypes, observed on minimal medium supplemented with various concentrations of calcium chloride. The experiment was repeated independently three times, yielding similar results. (b) Quantification of root span. Seedlings of the genotypes indicated were grown on minimal medium supplemented with various salt concentrations. At least 15 seedlings were measured per genotype. Seedlings of each genotype were randomized and distributed on at least three plates. Data points represent the mean ± SD from one representative experiment. The experiment was repeated independently three times, yielding similar results. Controls for chloride ions and additional salts are presented in Supporting Information Fig. S3.

1966). Addition of $MgSO_4$ and $MgCl_2$ caused a higher root span of Col-0 seedlings at 0.5–1 mM and a strong root growth inhibition above these concentrations, but neither salt had an effect on *mlo4*/*mlo11*-mediated root curling (Supporting Information Fig. S3b,c). Taken together, it appears that the suppressive effect on *mlo4*/*mlo11*-conditioned root curling is not due to osmotic conditions or presence of the Cl^- anion, but rather conferred by the chemically related bivalent cations Ca^{2+} and Sr^{2+}.

Exogenous application of ethylene glycol tetraacetic acid (EGTA) affects *mlo4* root growth

We next tested how presence of the Ca^{2+} chelator EGTA affects root growth patterns of Col-0 wild-type and *mlo4* seedlings. We observed that root span of Col-0 seedlings shortened with increasing (from 0 to 1 mM) EGTA concentrations, whereas roots of *mlo4* mutant seedlings showed the opposite behaviour, resulting in a partial loss of root curling (Fig. 6). Together with the data of exogenous $CaCl_2$ application (see above and Fig. 5), this finding suggests that *mlo4*-conditioned root coils require a tight balance of Ca^{2+} ions with too high or too low Ca^{2+} concentrations interfering with aberrant *mlo4* thigmomorphogenesis.

Differing requirements for root curling in accession Landsberg *erecta* and *mlo4* mutants

Arabidopsis ecotypes differ in their degree of natural root curvature on artificial substrates. Accession Landsberg *erecta* (L-*er*) shows pronounced root curling in these conditions (Chen *et al.* 2009), yielding a root span that is consistently smaller than that of Col-0. To find out whether root bending in L-*er* and *mlo4* mutants might be mechanistically related, we assessed the root growth pattern of these genotypes in comparison to Col-0 in the physiological conditions that were found to strongly modulate the *mlo4* phenotype, that is, at basic pH (pH 8.8 and 10.4) and elevated Ca^{2+} concentrations (10 mM). While consistent with our previous experiments (Figs 4 & 5), root curling of *mlo4* seedlings was compromised in these conditions, root coiling of L-*er* persisted on media with high pH, but not at the elevated Ca^{2+} concentration (Fig. 7a). However, the latter phenotype did not translate into a statistically significant difference in root span (Fig. 7b). These results suggest that the molecular mechanisms underlying the *mlo4* root spirals differ from or only partly overlap with those conferring root bending in L-*er*.

Gravistimulation reversibly overrides the aberrant thigmomorphogenic response of *mlo4* mutants

In wild-type plants, a mechanism of gravitropic resetting of directional root tip growth exists that is triggered by touch stimulation from encountered physical barriers (Massa & Gilroy 2003). We were interested to find out whether this mechanism also operates in the *mlo4* mutant, and if so,

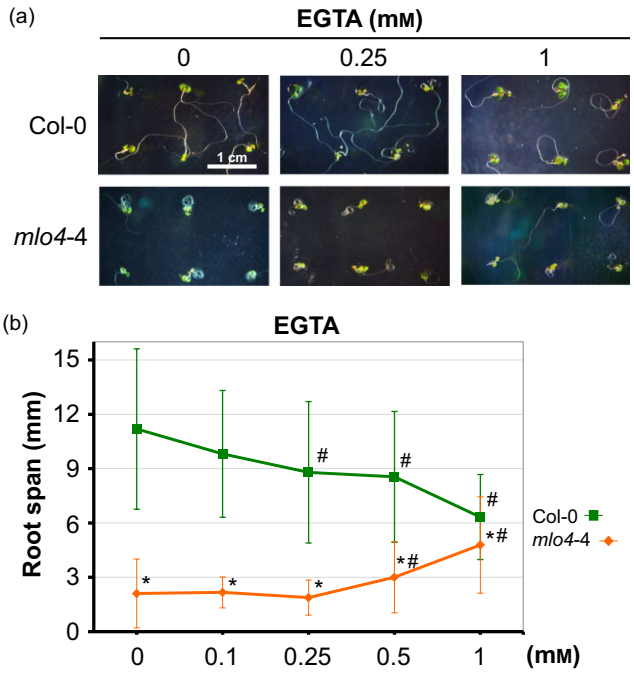

Figure 6. Exogenous application of ethylene glycol tetraacetic acid (EGTA) affects *mlo4* root curling. (a) Representation of the phenotypes of indicated genotypes, observed on minimal medium supplemented with various concentrations of EGTA. The experiment was repeated independently twice, yielding similar results. (b) Quantification of root span. Seedlings of the indicated genotypes were grown on minimal medium supplemented with various salt concentrations. At least 30 seedlings were measured per genotype. Seedlings of each genotype were randomized and distributed on at least three plates. Data points represent the mean ± SD from one representative experiment. An asterisk (*) denotes a statistically significant difference ($P < 0.05$, Student's *t*-test) from Col-0 in a given condition, a hash (#) signifies a statistically significant difference ($P < 0.05$, Student's *t*-test) from standard conditions (0 mM EGTA). The experiment was repeated independently twice, yielding similar results. Note that higher EGTA concentrations prevented seed germination (10 mM) or led to stunted roots (2.5 mM; data not shown).

whether this system is sufficient to suppress/override touch-induced root curling in *mlo4* mutants. To test this possibility, we designed two complementary experimental settings in which the otherwise constant touch stimulation would be alleviated at some point (Fig. 8).

The first experimental set-up was inspired by a previous work from Okada & Shimura (1990), who originally reported reversible thigmostimulation by plate tilting. Besides Col-0 wild-type and the *mlo4* mutant, we included the *eir1* (*pin2*) mutant, which is defective in the auxin efflux carrier PIN2, as an additional (agravitropic) control (Luschnig *et al.* 1998). We observed that during the first (horizontal) phase of growth, seedlings of all genotypes tested grew through the minimal medium and touched the bottom of the plate. Col-0 and *eir1* seedlings looked similar with relatively straight roots growing in random directions, whereas roots of the *mlo4* mutant formed first characteristic root coils. For the next stage, plates were turned and placed vertically. Col-0 control

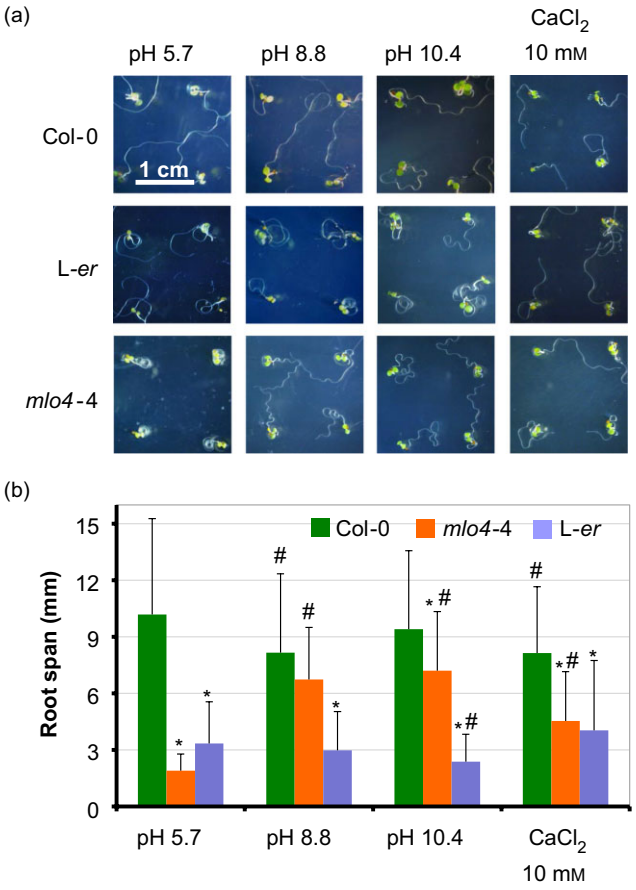

Figure 7. Differing requirements for root curling in accession Landsberg *erecta* and *mlo4* mutants. (a) Representation of the phenotypes of indicated genotypes, observed on minimal medium with different pH or 10 mM calcium chloride. Seedlings of each genotype were randomized and distributed on at least three plates. The experiment was repeated independently three times, yielding similar results. (b) Quantification of root span. Seedlings of the indicated genotypes were grown on minimal medium supplemented with various salt concentrations. At least 30 seedlings were measured per genotype. Seedlings of each genotype were distributed on at least three plates. Data points represent the mean ± SD from one representative experiment. An asterisk (*) denotes a statistically significant difference ($P < 0.05$, Student's *t*-test) from Col-0 in a given condition, a hash (#) signifies a statistically significant difference ($P < 0.05$, Student's *t*-test) from standard conditions (pH 5.7). The experiment was repeated independently three times, yielding similar results.

plants responded to the applied change in the plants' orientation to the gravity field and all roots grew downwards, whereas roots of *eir1* seedlings did not respond to the changed gravity vector and continued to grow in random directions. Interestingly, the root curling of *mlo4* mutant seedlings was suppressed and roots extended downwards following the gravity vector. In the final stage, when plates were placed back horizontally, roots of the Col-0 and *eir1* seedlings continued to grow in the previously established directions, whereas *mlo4* root curling was restored (Fig. 8b,c,d).

In the second experimental design, *mlo4* mutant roots followed the gravity vector towards a physical barrier embedded in the minimal medium, where they formed the characteristic root spirals (Fig. 8e). Some of the individuals extended the root curls beyond the border of the barrier, where root tips bended and again followed gravity until they

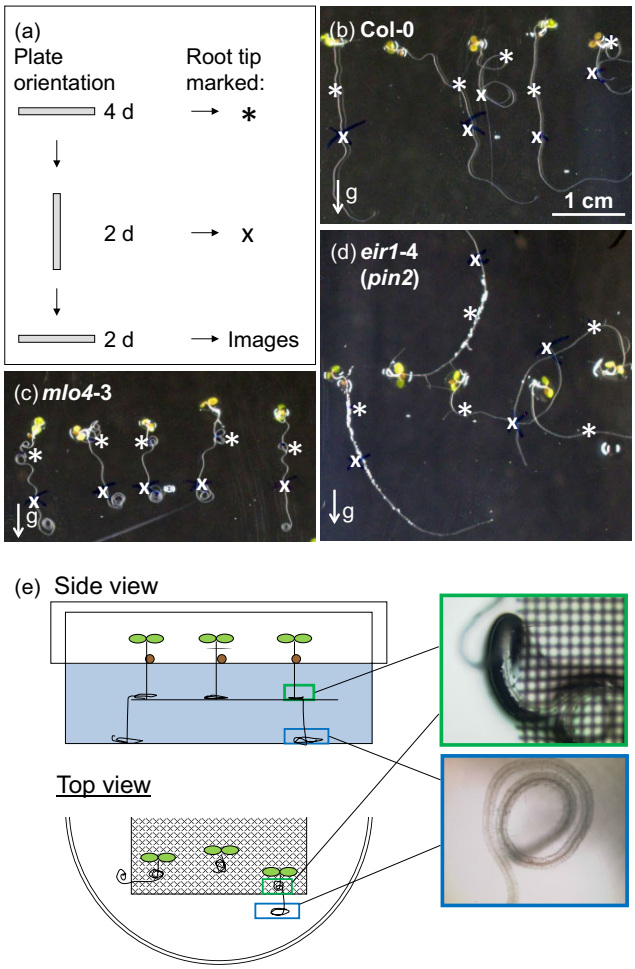

Figure 8. Gravistimulation reversibly overrides the aberrant thigmomorphogenic response of *mlo4* mutants. (a, d) Seedlings of the indicated genotypes were grown on the minimal medium for eight days with the changes in the plate orientation as schematically illustrated in (a). Asterisks (*) mark the position of the root tip after 4 d of horizontal growth, just before placing the plate in a vertical position. The crosses (x) mark the position of the root tip at the end of the vertical growth phase, just before returning the plate in the horizontal position. The vertical arrow indicates the direction of the gravity vector (*g*) during this phase. Images were taken 2 d after the second round of horizontal growth. Similar results were obtained when the vertical growth phase was in darkness. The experiment was repeated twice. Images are at the same scale. (e) Schematic drawing of the experimental set-up. The *mlo4* mutant was grown on minimal medium with an embedded physical barrier for root growth. A nylon mesh (72 μm^2 pore size) was placed on the first layer of minimal medium and then a second layer was poured on top, resulting in the embedded barrier for root growth. Boxed close-ups indicate root curls formed on the nylon mesh (green box; at the edge of the nylon mesh the root grows downwards to the bottom of the plate) and root curls formed on the bottom of the plate (blue box; the background haze results from the nylon mesh above).

reached the bottom of the plate. Roots of seedlings arriving at the bottom experienced a second tactile stimulus, which resulted in a second phase of aberrant root thigmotropism (Fig. 8e). Taken together, we observed in both experimental set-ups that *mlo4*-conditioned root curling can be overridden by a gravitropic stimulus and reinstated upon a second tactile cue. We thus conclude that the aberrant thigmotropism of *mlo4* roots is reversible and restricted to circumstances of continuous mechanostimulation by an impenetrable barrier.

Microtubules shape the extent and directionality of root curling

Among other mechanisms, plants regulate directional growth through the cellulose/microtubule machinery (Himmelspach *et al*. 1999; Wasteneys & Yang 2004). Missense or deletion mutants of α-tubulins or microtubule-associated proteins can cause abnormal microtubule arrays, which may result in helical growth in *A. thaliana* (Ishida *et al*. 2007). Here, we used two such mutants in *α-tubulin4*, *tua4*^{M268I} and *tua4*$^{S178\Delta}$, which on tilted agar surfaces are characterized by exaggerated left- or right-handed slanting, respectively (Ishida *et al*. 2007), to study their impact on *mlo4*- and *mlo11*-conditioned root thigmomorphogenesis.

We first quantitatively assessed the directionality of root curling of the *mlo4* and *mlo11* single mutants and the *mlo4 mlo11 mlo14* triple mutant. Both *mlo4* alleles tested showed no preference in root curling direction (ca. 30–40% curling clock- and counterclockwise) and a considerable number of *mlo4* roots (ca. 20–30%) changed directionality during growth. By contrast, *mlo11* roots showed a slight preference for clockwise root curling but a similar percentage of roots changing their direction (~30%) compared to *mlo4*. The *mlo4 mlo11 mlo14* triple mutant exhibited the most consistent root growth patterns, with ca. 40–45% curling clockwise and counterclockwise and only 12% that changed root growth direction (Fig. 9a).

When grown on minimal medium, the *α-tubulin* mutants, *tua4*^{M268I} and *tua4*$^{S178\Delta}$, developed roots that were very similar to those of Col-0 plants (Fig. 9b). Analysis of the double mutants showed that the *tua4*$^{S178\Delta}$ mutation seems to exaggerate the *mlo4* phenotype, often resulting in rollercoaster-like root growth patterns (Fig. 9c and Supporting Information Fig. S4e and Table S3). However, root growth directionality was not affected in this double mutant. By contrast, in the *mlo11* background, the *tua4*$^{S178\Delta}$ mutation resulted in roots that grow in a wavy manner on the bottom of the plates, very often changing direction and only rarely forming root curls similar to those observed in a *mlo11* single mutant (Fig. 9c and Supporting Information Fig. S4d,g,h and Table S3).

The other tubulin mutant tested, *tua4*^{M268I}, induced different phenotypic alterations. The *mlo4*-4 *tua4*^{M268I} double mutant formed nearly exclusively anti-clockwise root curls, which were more homogenous than those of the *mlo4* single mutant. By contrast, the *mlo11*-4 *tua4*^{M268I} double mutant lost the tight spiral-like root curling pattern and exhibited wide

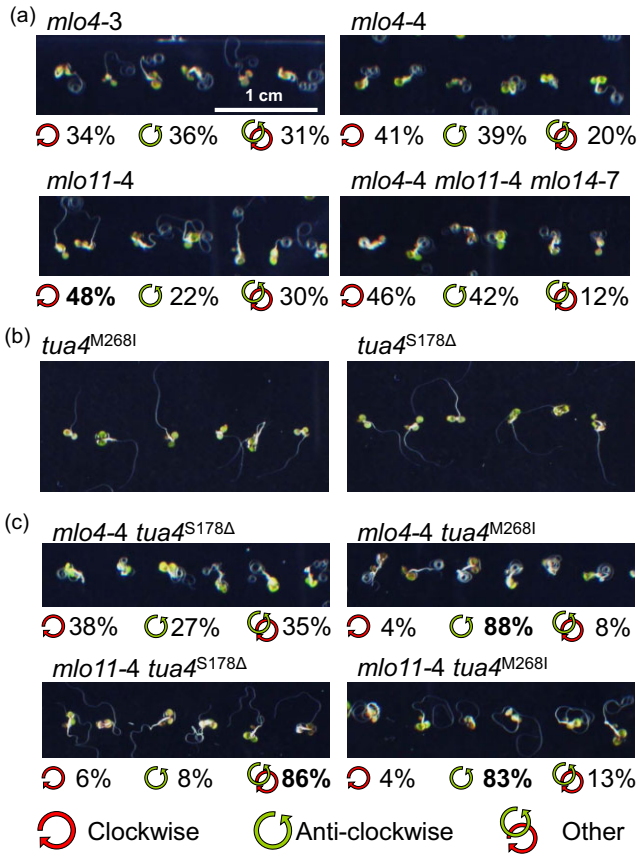

Figure 9. Modulation of root curling direction of *mlo4* and *mlo11* mutants by mutations in the gene coding for α-tubulin 4 (*TUA4*). The visual phenotype of the various *mlo* (a), *tua4* (b) and *mlo tua4* (c) mutants is shown. Quantification of the root curling direction (indicated by the code below the micrographs) is based upon at least 100 seedlings, randomized on seven plates. Seedlings were classified as clockwise or anti-clockwise, when the root observed from the bottom of the plate was exclusively bending in clockwise or anti-clockwise direction (for examples, see Supporting Information Fig. S4a,c, respectively). Secondary loops were allowed if there was no change in directionality (see Supporting Information Fig. S4b). All other cases were classified as 'other'. Detailed quantification is provided in Supporting Information Table S3. The experiment was repeated twice (c) or three times (a) with similar results. Additional characterization of the *mlo tua4* double mutants is presented in Supporting Information Fig. S4.

anti-clockwise curls (Fig. 9c and Supporting Information Fig. S4f and Table S3). In summary, both *α-tubulin4* mutants affected *mlo4*- and *mlo11*-conditioned root curling, indicating that aberrant root thigmomorphogenesis of *mlo4* and *mlo11* mutants is influenced by microtubule architecture and function.

Intact graviperception and polar auxin transport are required for *mlo4*-mediated root curling

To identify additional components regulating root curling in *mlo4* mutants, we performed a forward genetic suppressor

Table 1. *mlo4*-3 *rcs* double mutants that show suppression of the *mlo4* root curling phenotype

Genotype	Gravitropic responses			Auxin sensitivity	Suppressor gene	Segregation in F_2 generation of test cross with *mlo4*-1 (Ws-0) (curly:straight)
	Root	Shoot	Hypocotyl			
mlo4-3	WT	WT	WT	WT	n.a.	n.a.
mlo11-4	WT	WT	WT	WT	n.a.	n.a.
mlo4-3 rcs1	Delayed	WT	Non-responsive	WT	*PGM1* (At5g51820)	~3:1
mlo4-3 rcs2	Delayed	Non-responsive	Non-responsive	WT	*PGM1* (At5g51820)	~3:1
mlo4-3 rcs3	Delayed	WT	Non-responsive	WT	*PGM1* (At5g51820)	~3:1
mlo4-3 rcs4	Non-responsive	WT	Delayed	Altered	*AXR4* (At1g54990)	~3:1
mlo4-3 rcs5	WT	WT	WT	WT	n.a.	n.t.
mlo4-3 rcs6	WT	WT	WT	WT	n.a.	n.t.
mlo4-3 rcs7	WT	WT	WT	WT	n.a	n.t.
mlo4-3 rcs8	Delayed	WT	Delayed	Altered	n.a.	n.t.
mlo4-3 rcs9	Delayed	WT	Delayed	Non-responsive	n.a.	n.t.

n.a., not applicable; n.t., not tested; WT, wild-type-like.

screen. We monitored 14.100 M_2 seedlings of EMS-mutagenized *mlo4*-3 seeds and scored for seedlings that lack the characteristic *mlo4*-associated root spirals when grown on minimal medium. We identified nine root curling suppressor mutants (*rcs*) that showed a robust and heritable suppression of *mlo4*-associated root curling. Physiological characterization of the nine suppressor *mlo4*-3 *rcs* double mutants revealed that six exhibit altered gravitropic responses of the root, the hypocotyl or the shoot, and that among these six, three are also affected with regard to auxin sensitivity of root growth (Table 1, Fig. 10a,b and Supporting Information Fig. S5). The nine *mlo4 rcs* double mutants (in the *mlo4*-3 ecotype Col-0 background) were crossed to the *mlo4*-1 mutant (ecotype Ws-0) to generate segregating populations for map-based gene cloning (see the Materials and Methods section for details). The mutation in *rcs2* was initially mapped on the long arm of chromosome 5 to a 140 kb interval that comprises 35 genes. We then followed a candidate gene approach and identified a single nucleotide exchange in the *PHOSPHOGLUCOMUTASE1* gene (*PGM1*; At5g51820) as the causative mutation in *rcs2* (Fig. 10c). *PGM1* encodes a plastid isoform of phosphoglucomutase, which catalyses a key step in starch biosynthesis; accordingly, *pgm1* mutants typically lack starch granules in root statholiths and are delayed in the gravitropic response (Vitha *et al*. 2000). We assessed the presence of starch-containing statholiths in the nine suppressor mutants and found that *rcs2* and two additional mutants lack positive Lugol staining in seedling root tips (Fig. 10d). We therefore hypothesized that besides *rcs2*, also *rcs1* and *rsc3* might be defective in *PGM1*, which was subsequently confirmed by DNA sequencing (Fig. 10c). Assuming a defect in the auxin signalling pathway of the *rcs4* seedlings (Fig. 10b), we similarly cloned the *AXR4* gene (At1g54990) by combining genetic mapping and candidate gene sequencing. Sequence analysis of the *AXR4* locus in *rcs4* revealed a single nucleotide exchange resulting in a premature stop codon and a predicted truncated protein (Fig. 10c). The suppressor role of *AXR4* in *mlo4*-conditioned root thigmomorphogenesis was validated by an independently generated double mutant on the basis of a second *axr4* allele (*axr4*-2). Since AXR4 regulates the subcellular localization of the AUX1 auxin influx carrier (Dharmasiri *et al*. 2006), we hypothesized that an *aux1* mutant might also suppress the *mlo4* root curling phenotype, which was indeed the case (Fig. 10e). Taken together, the findings of the genetic suppressor screen indicate crucial roles for graviperception and auxin transport in the expression of aberrant root thigmomorphogenesis in the *mlo4* mutant.

DISCUSSION

Is the phenotype of *mlo4* and *mlo11* mutants unique?

We used a comprehensive set of mutants affected in root growth pattern or development to find out whether any of these mutants recapitulates the root thigmomorphogenesis defect of *mlo4* and *mlo11* seedlings (Fig. 1 and Supporting Information Table S1 and Fig. S1). While a few mutants showed some degree of root curling, none faithfully and consistently phenocopied the tight root spirals of *mlo4* and *mlo11* plants. This does not necessarily indicate that the root curling phenotype is a unique feature of *mlo4* and *mlo11* mutants. Even though the mutants under study were carefully selected for their potential to cause a similar phenotype as *mlo4* and *mlo11* mutants, they represent only a subjective subset of the genes known to govern root development and/or growth behaviour. We also cannot draw any conclusions for the mutants that were severely affected in root elongation in our experimental conditions (e.g. *erh2*-1 and *wvd2*-1). Furthermore, most of the lines tested were mutants in single genes; thus, genetic redundancy may mask any clear effects. Finally, we cannot disregard the possibility that the genes tested in this study act as suppressors of *mlo4*/*mlo11*-

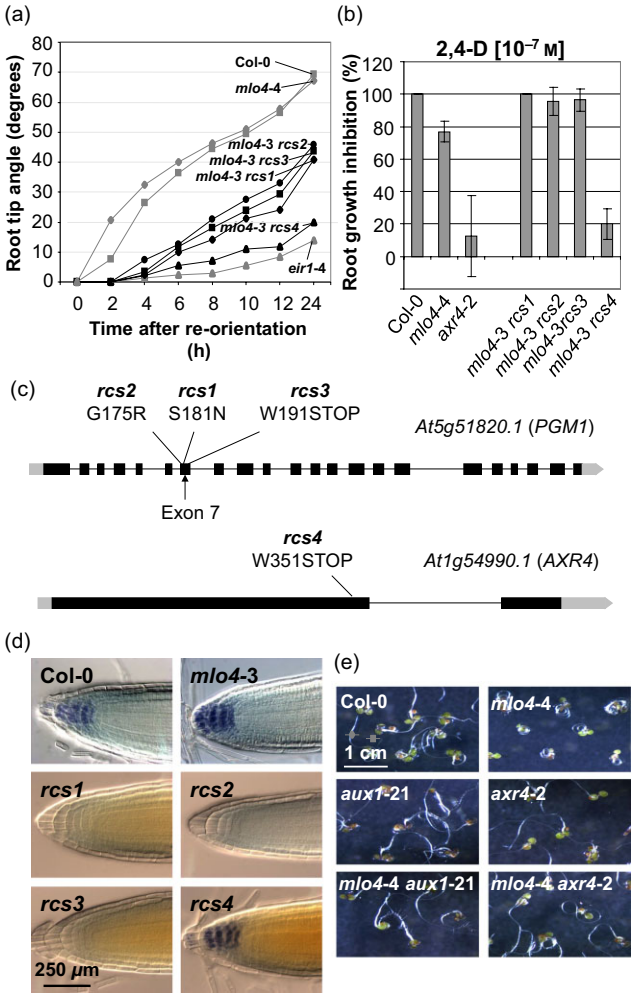

Figure 10. Characterization of *mlo4 rcs* root curling suppressor mutants. (a) Kinetics of root gravitropism after a 90° re-orientation. Eight-day-old seedlings were subjected to gravistimulation in the darkness. Root curvatures after (90° re-orientation with respect to the gravity vector) of the seedling were measured every 2 h for a total of 12 h. Values represent mean (for visibility without error bars) on the basis of 4–8 seedlings per genotype. The experiment was repeated twice with similar results. (b) Results of the auxin sensitivity test. After 5 d of growth on vertical plates containing Murashige and Skoog (MS) medium, seedlings were transferred to vertical plates with MS medium containing various concentrations of 2,4-D (2,4-dichlorophenoxyacetic acid). Root length elongation was measured 3 d later. Data for 10^{-7} mM 2,4-D are presented. Bars represent the mean ± SD on the basis of four seedlings per genotype. The experiment was repeated three times with similar results. (c) *PGM1* (upper panel) and *AXR1* (lower panel) gene structure, respectively, and mutations identified in the suppressor mutants. Boxes indicate exons, connecting lines introns. Untranslated 5′ and 3′ regions are coloured in grey. Approximate positions of amino acid exchanges are indicated based upon the *TAIR10* gene structure and sequencing. (d) Visualization of starch grains in the root tip by Lugol staining. (e) Representation of the phenotypes of indicated genotypes grown on horizontal plates with minimal medium.

conditioned root curling. Nonetheless, the outcome of this survey is in line with the preliminary results from an ongoing forward genetic screen aiming at the identification of EMS-induced mutants that phenocopy the *mlo4*/*mlo11*-like root growth pattern. Apart from additional *mlo11* alleles, this screen did not reveal any phenocopy mutant so far.

Of the mutants tested in this study, only the *wag1*-1 *wag2*-1 double mutant showed root spirals that were, to some extent, similar to those of *mlo4*, although the severity and penetrance of the phenotype was considerably lower in the double mutant than in the *mlo4* single mutant (Fig. 1 and Supporting Information Table S1). This result is notable, since both *WAG1* (At1g53700) and *WAG2* (At3g14370) are tightly co-expressed with *MLO4* according to the ATTED-II co-expression database (http://atted.jp/; Obayashi *et al.* 2009). A high degree of co-expression was previously found to represent a good indicator for functioning of genes in the same biological process (Wei *et al.* 2006; Humphry *et al.* 2010; Obayashi & Kinoshita 2010). The phenotype of the *wag1 wag2* double mutant will require closer inspection to find out whether it represents a genuine phenocopy of the *mlo4* mutant or just a superficially related phenotype.

WAG1 and *WAG2* encode serine/threonine kinases of the PsPK3-type. Together with the two closely related family members PINOID (PID; At2g34650) and PID2 (At2g26700), WAG1 and WAG2 form a separate clade in the phylogenetic tree of the PsPK3 kinases (Santner & Watson 2006). PINOID is supposed to act as a positive regulator of auxin transport and a negative regulator of auxin signalling (Christensen *et al.* 2000). It has been shown to interact with the Ca^{2+}-binding proteins TCH3 (a calmodulin-like protein implicated in mechanoresponses; Braam & Davis 1990) and PBP1 (a small protein with a single Ca^{2+}-binding EF-hand; Benjamins *et al.* 2003). It was therefore suggested that TCH3 and PBP1 regulate the activity of PID in response to changes in Ca^{2+} levels. Notably, *PINOID* is also co-expressed with *MLO4* according to the ATTED-II co-expression database. If *WAG1* and *WAG2* indeed function in the *MLO4* pathway (see previous discussion), then the incomplete penetrance of the root coiling phenotype of the *wag1*-1 *wag2*-1 double mutant might be attributable to potential genetic redundancy of *WAG1* and *WAG2* with *PINOID* and possibly also *PID2* in this process.

Physiological parameters modulating *mlo4*/*mlo11*-dependent root curling

We found that the formation of root coils in *mlo4* and *mlo11* mutants occurs independently of light or darkness (Fig. 2). This result seems surprising in the light of the data from our previous study (Chen *et al.* 2009) and probably is the consequence of the longer growth period allowed for in the present work. Although roots are underground organs, they are able to perceive light penetrating into the soil (Galen *et al.* 2007a,b; Kutschera & Briggs 2012). Light perception by roots is important for many developmental aspects as well as for positive gravitropism (Feldman & Gildow 1984) or drought tolerance (Galen *et al.* 2007a). The fact that *mlo4* and *mlo11* mutant plants have the capability to form root coils in dark-

ness indicates that, contrary to previous belief, the phenotype of these mutants is not associated with a defect in either perceiving or responding to a light-associated or photosynthesis-derived signal.

Consistent with their well-documented function in the modulation of polar auxin transport (Stenlid 1976; Santelia *et al*. 2008), results from previous pharmacological inhibitor experiments pointed at a potential role for flavonoids in the establishment of the aberrant thigmoresponses in *mlo4* and *mlo11* mutants. However, on the basis of genetic experiments, we found that *mlo4/mlo11*-like aberrant root curvature is neither suppressed nor induced by the absence of endogenous flavonoids (Fig. 3). Thus, interference with auxin transport might not be the primary causative effect of the flavonoids (karanjin, robustic acid and prunetin) originally identified in the pharmacological screen.

We have shown here that root thigmomorphogenesis defect in *mlo4* and *mlo11* mutants observed *in vitro* is pH-dependent and can be suppressed by a high pH (>6.5) of the surrounding medium (Fig. 4). This might be simply a cytotoxic effect, as changes in pH can have a severe impact on protein folding and activity. While cellular pH is well buffered at ca. 7.5 in an external pH range from ca. 4.5 to 7.5, external pH values lower than 4.5 and higher than 7.5 cause a proportional decrease (owing to insufficient H^+ ATPase activity) or increase (via a passive influx of $[OH^-]$ ions), respectively, of cytoplasmic and vacuolar pH (Gout *et al*. 1992). It was recently shown that mechanical stimulation of Arabidopsis roots is associated with apoplastic alkalinization and cytoplasmic acidification. These alterations in pH are dependent on Ca^{2+} influx, as application of lanthanum, a non-selective Ca^{2+} channel blocker, inhibits the respective pH changes (Monshausen *et al*. 2009). A possible explanation for the loss of the *mlo4*/*mlo11* root curling phenotype on high pH medium could be the effect of such pH values on auxin transport. In physiological conditions, the apoplastic pH is ~5.5, which allows IAAH, the protonated form of the natural auxin, indole acetic acid (IAA), to diffuse across the plasma membrane. It becomes negatively charged IAA^- in the cytoplasm and is consequently trapped intracellularly (Weijers & Friml 2009). An increase in extracellular pH may result in lower intracellular auxin levels by shifting the extracellular IAAH pool to the deprotonated form, which cannot cross the plasma membrane.

We discovered that elevated extracellular Ca^{2+} (and Sr^{2+}) levels suppress the root curling phenotype of *mlo4*, *mlo11* and *mlo4 mlo11 mlo14* mutants (Fig. 5 and Supporting Information Fig. S3). Exogenous application of Ca^{2+} affected the *mlo11* mutant at a lower concentration (2.5 mM) than the *mlo4* and *mlo4 mlo11 mlo14* mutant (10 mM; Fig. 5). This result is consistent with the previously described more robust and more consistent root coiling of the *mlo4* mutant as compared to *mlo11*. Notably, also lowering the apoplastic Ca^{2+} concentrations by exogenous application of EGTA partially compromised *mlo4* root curling (Fig. 6). The suppressive effect of altered Ca^{2+} levels might be due to either the interference with (a) *MLO*/*mlo*-specific signalling pathway(s) or the rather indirect consequence of perturbation of the polar auxin transport machinery. Accumulating evidence linking Ca^{2+} signalling to *MLO*/*mlo* function (Bayles & Aist 1987; Kim *et al*. 2002; Bhat *et al*. 2005; Freymark *et al*. 2007; Kobayashi *et al*. 2007; Kim & Hwang 2012; see the Introduction section for details) may argue for the former scenario. However, pH homoeostasis, Ca^{2+} signalling and polar auxin transport appear to be highly interconnected processes (Yang & Poovaiah 2000; Benjamins *et al*. 2003; Steinacher *et al*. 2012). It was recently shown that auxin regulates root curvature and associated growth-related apoplastic pH changes through a Ca^{2+}-dependent signalling pathway (Monshausen *et al*. 2011). In addition, changes in external pH result in massive changes of gene expression patterns, including transcript levels of auxin signalling genes. Notably, a marked over-representation of motifs related to Ca^{2+} signalling was detected in the promoters of the pH-responsive genes (Lager *et al*. 2010). Given these observations, it is at present impossible to decide whether the effect of exogenous Ca^{2+} is *MLO*/*mlo*-specific or the indirect result of perturbation of the complex Ca^{2+}/pH/auxin network. In any way, the molecular mechanisms governing *mlo4*-dependent root curling appear to be different or only partly overlap with that conferring root curvature in the Arabidopsis accession Landsberg *erecta* (Fig. 7).

Genes that modulate *mlo4*/*mlo11*-dependent root curling

Our unbiased and targeted genetic studies identified *PGM1*, *AXR4*, *AUX1* and *TUA* as components that control the *mlo4* root curling response (Figs. 9 & 10). The contribution of *AXR4* and *AUX1* is not surprising, given the well-known role of auxin in plant growth and different tropic responses. Accordingly, mutations in the auxin efflux carrier gene *EIR1*/*AGR1*/*PIN2* were previously shown to suppress *mlo4*-associated root coiling (Chen *et al*. 2009). Mutants affected in the auxin transport machinery typically exhibit altered gravitropic responses, a phenotype shared with Arabidopsis seedlings defective in *PGM1*, another gene identified in our forward genetic screen. *PGM1* encodes a phosphoglucomutase, an enzyme required for starch biosynthesis. Without starch, amyloplasts in the columella of root cap cells sediment at a slower rate in response to gravity resulting in delayed gravitropic root bending (Vitha *et al*. 2000). Thus, proper root gravitropic responses appear to be crucial for the formation of *mlo4* root spirals. As future tasks, it will be interesting to investigate the effect of mutations in *PGM1* on *mlo11*-conditioned root curling and to clone the genes mutated in suppressor double mutants *mlo4 rcs5*, *mlo4 rcs6* and *mlo4 rcs7*, in which gravitropic responses and auxin sensitivity appear to be unaltered (Table 1).

The *tua4*^{M268I} and *tua4*$^{S178\Delta}$ mutants are characterized by exaggerated left- or right-handed slanting, which correlates with the arrangement of cortical microtubules (Ishida *et al*. 2007). However, although these single mutants behave as wild-type seedlings in our assay conditions, they have a striking impact on *mlo4*/*mlo11*-dependent root curling (Fig. 9). It is well known that tubulin is one of the downstream execu-

tion machinery elements recruited to shape directional growth by determining cellulose deposition (Himmelspach *et al*. 1999; Paradez *et al*. 2006). Accordingly, mutants with defects in tubulin subunits *TUA4* and *TUA6* (Thitamadee *et al*. 2002; Ishida & Hashimoto 2007; Ishida *et al*. 2007) or other microtubular components (mutants *spr1* and *spr2*, Furutani *et al*. 2000; Sedbrook *et al*. 2004; Shoji *et al*. 2004; *eb1*, Bisgrove *et al*. 2008; Gleeson *et al*. 2012; *sku6*, Sedbrook *et al*. 2004; or *wvd2*, Perrin *et al*. 2007) were shown to be affected in root growth responses. Some of these mutants, for example, *wvd2*-1 and *wdl1*-4, which show suppressed root waving and left-handed root slanting on tilted agar plates (Yuen *et al*. 2003), were tested in our survey for *mlo4* phenocopy mutants (Fig. 1), but did not show an obvious phenotype in these conditions. It would be interesting in the context of future work to combine these mutants (*eb1*, *spr1*, *spr2*, *wvd2*, *wdl1*) with *mlo4* or *mlo11* mutations to find out whether defects in microtubular components generally affect *mlo4*/*mlo11*-conditioned root coiling.

Do MLO proteins function in plant cell wall integrity sensing?

Physiological characterization and genetic analysis performed in this study indicate that pH homoeostasis, Ca^{2+} signalling, polar auxin transport, intact gravitropism and microtubular function are components of root thigmomorphogenesis. Many, if not all, of these mechanisms appear to be functionally interconnected with each other. The emerging picture is that auxin gradients govern the responses to thigmomorphogenic cues, which are then translated via the microtubular cytoskeleton (and thus likely the positioning of the cellulose biosynthesis machinery) in altered directional growth responses. Exogenous alterations in pH and $[Ca^{2+}]$, as well as inappropriate gravitropic response levels, may simply indirectly modulate the polar auxin transport machinery. Notably, a recent study implicated an Arabidopsis calmodulin-like gene (*CML24*; one of the *TCH* genes identified as mechanosensitive; Braam & Davis 1990) in the regulation of root mechanoresponses and cortical microtubule orientation, thereby also linking Ca^{2+} signalling and microtubule function to root thigmostimulation (Wang *et al*. 2011).

It still remains unknown how the physical stimulus is perceived and transduced to the auxin-dependent execution machinery and which role MLO proteins play in this process. As plasma membrane proteins, members of the MLO family might comprise components of the touch-sensing complex. A function in this context would be consistent with the phenotypes of other *mlo* mutants, such as the resistance to cell wall-penetrating powdery mildew fungi (Büschges *et al*. 1997; Consonni *et al*. 2006; Bai *et al*. 2008; Humphry *et al*. 2011) and the inability of the female gametophyte to perceive and/or interpret a pollen-derived (touch?) signal for fertilization (Kessler *et al*. 2010). Accumulating evidence indicates the existence of dedicated cell wall integrity sensing mechanisms in plants (Ringli 2010; Hamann 2012). Plasma membrane-resident transmembrane proteins represent prime candidates for having a function in sensing the cell wall status and transducing this information to the cytoplasm. Interestingly, functions of some proteins presently implicated in cell wall-related signalling and development comprise a similar set of activities (Ca^{2+} signalling, pH regulation and microtubule orientation; Ringli 2010) as those identified as crucial for *mlo4*-based thigmomorphogenesis in this study. However, the hypothesized function of MLO proteins as touch sensors and/or a well-defined link of MLO proteins to the cell wall integrity sensing system remain to be shown.

ACKNOWLEDGMENTS

We acknowledge Mark Estelle, Thorsten Hamann, Takashi Hashimoto, Alan M. Jones, Christian Luschnig, Yusuke Saijo and Ben Scheres for providing seeds of Arabidopsis mutants. We thank the MPIPZ Plant Cultivation Facility personnel for taking care of the plant material and Elmon Schmelzer for assistance with microscopy. This work was supported by funds from the Max Planck Society, an Erasmus Lifelong Learning Scholarship (D.M.G.), and by funds from the RWTH Aachen University.

REFERENCES

Anten N.P.R., Casado-Garcia R., Pierik R. & Pons T.L. (2006) Ethylene sensitivity affects changes in growth patterns, but not stem properties, in response to mechanical stress in tobacco. *Physiologia Plantarum* **128,** 274–282.

Bai Y.L., Pavan S., Zheng Z., Zappel N.F., Reinstädler A., Lotti C., & Panstruga R. (2008) Naturally occurring broad-spectrum powdery mildew resistance in a Central American tomato accession is caused by loss of *Mlo* function. *Molecular Plant-Microbe Interactions* **21,** 30–39.

Bayles C.J. & Aist J.R. (1987) Apparent calcium mediation of resistance of an *mL-o* barley mutant to powdery mildew. *Physiological and Molecular Plant Pathology* **30,** 337–345.

Benjamins R., Ampudia C.S.G., Hooykaas P.J.J. & Offringa R. (2003) PINOID-mediated signaling involves calcium-binding proteins. *Plant Physiology* **132,** 1623–1630.

Bhat R.A., Miklis M., Schmelzer E., Schulze-Lefert P. & Panstruga R. (2005) Recruitment and interaction dynamics of plant penetration resistance components in a plasma membrane microdomain. *Proceedings of the National Academy of Sciences of the United States of America* **102,** 3135–3140.

Bisgrove S.R., Lee Y.-R.J., Liu B., Peters N.T. & Kropf D.L. (2008) The microtubule plus-end binding protein EB1 functions in root responses to touch and gravity signals in *Arabidopsis*. *The Plant Cell* **20,** 396–410.

Braam J. & Davis R.W. (1990) Rain-induced, wind-induced, and touch-induced expression of calmodulin and calmodulin-related genes in Arabidopsis. *Cell* **60,** 357–364.

Buer C.S., Imin N. & Djordjevic M.A. (2010) Flavonoids: new roles for old molecules. *Journal of Integrative Plant Biology* **52,** 98–111.

Büschges R., Hollricher K., Panstruga R., Simons G., Wolter M., Frijters A., & Schulze-Lefert P. (1997) The barley *Mlo* gene: a novel control element of plant pathogen resistance. *Cell* **88,** 695–705.

Chehab E.W., Eich E. & Braam J. (2009) Thigmomorphogenesis: a complex plant response to mechano-stimulation. *Journal of Experimental Botany* **60,** 43–56.

Chehab E.W., Yao C., Henderson Z., Kim S. & Braam J. (2012) *Arabidopsis* touch-induced morphogenesis is jasmonate mediated and protects against pests. *Current Biology* **22,** 701–706.

Chen Z.Y., Noir S., Kwaaitaal M., Hartmann H.A., Wu M.J., Mudgil Y., . . . Jones A.M. (2009) Two seven-transmembrane domain MILDEW RESISTANCE LOCUS O proteins cofunction in *Arabidopsis* root thigmomorphogenesis. *The Plant Cell* **21,** 1972–1991.

Christensen S.K., Dagenais N., Chory J. & Weigel D. (2000) Regulation of auxin response by the protein kinase PINOID. *Cell* **100,** 469–478.

Consonni C., Humphry M.E., Hartmann H.A., Livaja M., Durner J., Westphal L., & Panstruga R. (2006) Conserved requirement for a plant host cell protein in powdery mildew pathogenesis. *Nature Genetics* **38,** 716–720.

Devoto A., Piffanelli P., Nilsson I., Wallin E., Panstruga R., Heijne G. & von Schulze-Lefert P. (1999) Topology, subcellular localization, and sequence diversity of the Mlo family in plants. *The Journal of Biological Chemistry* **274,** 34993–35004.

Devoto A., Hartmann H.A., Piffanelli P., Elliot C., Simmons C., Taramino G., & Panstruga R. (2003) Molecular phylogeny and evolution of the plant-specific seven-transmembrane MLO family. *Journal of Molecular Evolution* **56,** 77–88.

Dharmasiri S., Swarup R., Mockaitis K., Dharmasiri N., Singh S.K., Kowalchyk M., & Estelle M. (2006) AXR4 is required for localization of the auxin influx facilitator AUX1. *Science* **312,** 1218–1220.

Feldman L.J. & Gildow V. (1984) Effects of light on protein patterns in gravitropically stimulated root caps of corn. *Plant Physiology* **74,** 208–212.

Freymark G., Diehl T., Miklis M., Romeis T. & Panstruga R. (2007) Antagonistic control of powdery mildew host cell entry by barley calcium-dependent protein kinases (CDPKs). *Molecular Plant-Microbe Interactions* **20,** 1213–1221.

Furutani I., Watanabe Y., Prieto R., Masukawa M., Suzuki K., Naoi K., ... Hashimoto T. (2000) The SPIRAL genes are required for directional central of cell elongation in *Arabidopsis thaliana*. *Development (Cambridge, England)* **127,** 4443–4453.

Galen C., Rabenold J.J. & Liscum E. (2007a) Functional ecology of a blue light photoreceptor: effects of phototropin-1 on root growth enhance drought tolerance in *Arabidopsis thaliana*. *New Phytologist* **173,** 91–99.

Galen C., Rabenold J.J. & Liscum E. (2007b) Light-sensing in roots. *Plant Signaling and Behavior* **2,** 106–108.

Gleeson L., Squires S. & Bisgrove S.R. (2012) The microtubule associated protein END BINDING 1 represses root responses to mechanical cues. *Plant Science* **187,** 1–9.

Gout E., Bligny R. & Douce R. (1992) Regulation of intracellular pH values in higher plant cells. Carbon-13 and phosphorous-31 nuclear magnetic resonance studies. *The Journal of Biological Chemistry* **267,** 13903–13909.

Hamann T. (2012) Plant cell wall integrity maintenance as an essential component of biotic stress response mechanisms. *Frontiers in Plant Science* **3,** 77.

Himmelspach R., Wymer C.L., Lloyd C.W. & Nick P. (1999) Gravity-induced reorientation of cortical microtubules observed *in vivo*. *The Plant Journal* **18,** 449–453.

Humphry M., Bednarek P., Kemmerling B., Koh S., Stein M., Göbel U., & Panstruga R. (2010) A regulon conserved in monocot and dicot plants defines a functional module in antifungal plant immunity. *Proceedings of the National Academy of Sciences of the United States of America* **107,** 21896–21901.

Humphry M., Reinstädler A., Ivanov S., Bisseling T. & Panstruga R. (2011) Durable broad-spectrum powdery mildew resistance in pea *er1* plants is conferred by natural loss-of-function mutations in *PsMLO1*. *Molecular Plant Pathology* **12,** 866–878.

Ishida T. & Hashimoto T. (2007) An *Arabidopsis thaliana* tubulin mutant with conditional root-skewing phenotype. *Journal of Plant Research* **120,** 635–640.

Ishida T., Kaneko Y., Iwano M. & Hashimoto T. (2007) Helical microtubule arrays in a collection of twisting tubulin mutants of *Arabidopsis thaliana*. *Proceedings of the National Academy of Sciences of the United States of America* **104,** 8544–8549.

Jaffe M.J., Leopold A.C. & Staples R.C. (2002) Thigmo responses in plants and fungi. *American Journal of Botany* **89,** 375–382.

Johnson K.A., Sistrunk M.L., Polisensky D.H. & Braam J. (1998) *Arabidopsis thaliana* responses to mechanical stimulation do not require ETR1 or EIN2. *Plant Physiology* **116,** 643–649.

Kessler S.A., Shimosato-Asano H., Keinath N.F., Wuest S.E., Ingram G., Panstruga R. & Grossniklaus U. (2010) Conserved molecular components for pollen tube reception and fungal invasion. *Science* **330,** 968–971.

Kim D.S. & Hwang B.K. (2012) The pepper *MLO* gene, *CaMLO2*, is involved in the susceptibility cell-death response and bacterial and oomycete proliferation. *The Plant Journal* **72,** 843–855.

Kim M.C., Panstruga R., Elliott C., Müller J., Devoto A., Yoon H.W., ... Schulze-Lefert P. (2002) Calmodulin interacts with MLO protein to regulate defence against mildew in barley. *Nature* **416,** 447–450.

Kimbrough J.M., Salinas-Mondragon R., Boss W.F., Brown C.S. & Sederoff H.W. (2004) The fast and transient transcriptional network of gravity and mechanical stimulation in the Arabidopsis root apex. *Plant Physiology* **136,** 2790–2805.

Kobayashi I., Yamada M. & Kobayashi Y. (2007) Calcium ion promotes successful penetration of powdery mildew fungi into barley cells. *Journal of General Plant Pathology* **73,** 399–404.

Kutschera U. & Briggs W.R. (2012) Root phototropism: from dogma to the mechanism of blue light perception. *Planta* **235,** 443–452.

Lager I., Andréasson O., Dunbar T.L., Andreasson E., Escobar M.A. & Rasmusson A.G. (2010) Changes in external pH rapidly alter plant gene expression and modulate auxin and elicitor responses. *Plant, Cell & Environment* **33,** 1513–1528.

Lepiniec L., Debeaujon I., Routaboul J.M., Baudry A., Pourcel L., Nesi N. & Caboche M. (2006) Genetics and biochemistry of seed flavonoids. *Annual Review of Plant Biology* **57,** 405–430.

Leyser O. & Day S. (2003) *Mechanisms in Plant Development*. Blackwell, Oxford, Malden, MA, USA.

Luschnig C., Gaxiola R.A., Grisafi P. & Fink G.R. (1998) EIR1, a root-specific protein involved in auxin transport, is required for gravitropism in *Arabidopsis thaliana*. *Genes and Development* **12,** 2175–2187.

Malamy J.E. (2005) Intrinsic and environmental response pathways that regulate root system architecture. *Plant, Cell & Environment* **28,** 67–77.

Massa G.D. & Gilroy S. (2003) Touch modulates gravity sensing to regulate the growth of primary roots of *Arabidopsis thaliana*. *The Plant Journal* **33,** 435–445.

Migliaccio F. & Piconese S. (2001) Spiralizations and tropisms in *Arabidopsis* roots. *Trends in Plant Science* **6,** 561–565.

Miledi R. (1966) Strontium as a substitute for calcium in process of transmitter release at neuromuscular junction. *Nature* **212,** 1233–1234.

Monshausen G.B., Bibikova T.N., Weisenseel M.H. & Gilroy S. (2009) Ca^{2+} regulates reactive oxygen species production and pH during mechanosensing in *Arabidopsis* roots. *The Plant Cell* **21,** 2341–2356.

Monshausen G.B., Miller N.D., Murphy A.S. & Gilroy S. (2011) Dynamics of auxin-dependent Ca^{2+} and pH signaling in root growth revealed by integrating high-resolution imaging with automated computer vision-based analysis. *The Plant Journal* **65,** 309–318.

Nakagawa Y., Katagiri T., Shinozaki K. & Yamanaka T. (2007) *Arabidopsis* plasma membrane protein crucial for Ca^{2+} influx and touch sensing in roots. *Proceedings of the National Academy of Sciences of the United States of America* **104,** 3639–3644.

Obayashi T. & Kinoshita K. (2010) Coexpression landscape in ATTED-II: usage of gene list and gene network for various types of pathways. *Journal of Plant Research* **123,** 311–319.

Obayashi T., Hayashi S., Saeki M., Ohta H. & Kinoshita K. (2009) ATTED-II provides coexpressed gene networks for Arabidopsis. *Nucleic Acids Research* **37,** D987–D991.

Okada K., & Shimura Y. (1990) Reversible root tip rotation in Arabidopsis seedlings induced by obstacle-touching stimulus. *Science* **250,** 274–276.

Osmont K.S., Sibout R. & Hardtke C.S. (2007) Hidden branches: developments in root system architecture. *Annual Review of Plant Biology* **58,** 93–113.

Panstruga R. (2005) Serpentine plant MLO proteins as entry portals for powdery mildew fungi. *Biochemical Society Transactions* **33,** 389–392.

Paradez A., Wright A. & Ehrhardt D.W. (2006) Microtubule cortical array organization and plant cell morphogenesis. *Current Opinion in Plant Biology* **9,** 571–578.

Perrin R.M., Wang Y., Yuen C.Y.L., Will J. & Masson P.H. (2007) WVD2 is a novel microtubule-associated protein in *Arabidopsis thaliana*. *The Plant Journal* **49,** 961–971.

Ringli C. (2010) Monitoring the outside: cell wall-sensing mechanisms. *Plant Physiology* **153,** 1445–1452.

Santelia D., Henrichs S., Vincenzetti V., Sauer M., Bigler L., Klein M., & Martinoia E. (2008) Flavonoids redirect PIN-mediated polar auxin fluxes during root gravitropic responses. *The Journal of Biological Chemistry* **283,** 31218–31226.

Santner A.A. & Watson J.C. (2006) The WAG1 and WAG2 protein kinases negatively regulate root waving in Arabidopsis. *The Plant Journal* **45,** 752–764.

Sedbrook J.C., Ehrhardt D.W., Fisher S.E., Scheible W.R. & Somerville C.R. (2004) The Arabidopsis *SKU6*/*SPIRAL1* gene encodes a plus end-localized microtubule-interacting protein involved in directional cell expansion. *The Plant Cell* **16,** 1506–1520.

Shoji T., Narita N.N., Hayashi K., Hayashi K., Asada J., Hamada T., ... Hashimoto T. (2004) Plant-specific microtubule-associated protein

SPIRAL2 is required for anisotropic growth in Arabidopsis. *Plant Physiology* **136,** 3933–3944.
Steinacher A., Leyser O. & Clayton R.H. (2012) A computational model of auxin and pH dynamics in a single plant cell. *Journal of Theoretical Biology* **296,** 84–94.
Stenlid G. (1976) Effects of flavonoids on polar transport of auxins. *Physiologia Plantarum* **38,** 262–266.
Telewski F.W. (2006) A unified hypothesis of mechanoperception in plants. *American Journal of Botany* **93,** 1466–1476.
Thitamadee S., Tuchihara K. & Hashimoto T. (2002) Microtubule basis for left-handed helical growth in *Arabidopsis*. *Nature* **417,** 193–196.
Vitha S., Zhao L.M. & Sack F.D. (2000) Interaction of root gravitropism and phototropism in Arabidopsis wild-type and starchless mutants. *Plant Physiology* **122,** 453–461.
Wang Y.C., Wang B.C., Gilroy S., Chehab E.W. & Braam J. (2011) CML24 is involved in root mechanoresponses and cortical microtubule orientation in *Arabidopsis*. *Journal of Plant Growth Regulation* **30,** 467–479.
Wasteneys G.O. & Yang Y.B. (2004) New views on the plant cytoskeleton. *Plant Physiology* **136,** 3884–3891.
Wei H.R., Persson S., Mehta T., Srinivasasainagendra V., Chen L., Page G.P., . . . Loraine A. (2006) Transcriptional coordination of the metabolic network in Arabidopsis. *Plant Physiology* **142,** 762–774.
Weijers D. & Friml J. (2009) SnapShot: auxin signaling and transport. *Cell* **136,** 1172–e1.
Yamamoto C., Sakata Y., Taji T., Baba T. & Tanaka S. (2008) Unique ethylene-regulated touch responses of *Arabidopsis thaliana* roots to physical hardness. *Journal of Plant Research* **121,** 509–519.
Yamanaka T., Nakagawa Y., Mori K. & Kazuo I. (2010) MCA1 and MCA2 that mediate Ca^{2+} uptake have distinct and overlapping roles in Arabidopsis. *Plant Physiology* **152,** 1284–1296.
Yang T. & Poovaiah B.W. (2000) Molecular and biochemical evidence for the involvement of calcium/calmodulin in auxin action. *Journal of Biological Chemistry* **275,** 3137–3143.
Yuen C.Y.L., Pearlman R.S., Silo-Suh L., Hilson P., Carroll K.L. & Masson P.H. (2003) WVD2 and WDL1 modulate helical organ growth and anisotropic cell expansion in Arabidopsis. *Plant Physiology* **131,** 493–506.

Received 22 April 2013; accepted for publication 18 March 2014

SUPPORTING INFORMATION

Additional Supporting Information may be found in the online version of this article at the publisher's web-site:

Figure S1. Quantification of root span in mutants affected in root architecture grown on minimal medium. Quantification of root span was performed with 7-day-old seedlings. Columns represent the mean ± SD of 10–20 roots measured per genotype. The horizontal dashed line was set to indicate the mean root span of the *mlo4*-4 *mlo11*-4 *mlo14*-7 triple mutant. An asterisk denotes a statistically significant difference ($P < 0.05$, Student's *t*-test) from Col-0. For each genotype, the experiment was repeated at least three times, yielding similar results.

Figure S2. Phenotypes of root architecture mutants grown on minimal medium – additional alleles. Seedlings of the indicated genotypes were grown on horizontal plates with minimal medium. Pictures of representative seedlings were taken from above at 7 d after sowing and root span was measured. Quantification of *mlo4*-like root curling and details of tested mutants are given in Supporting Information Table S1. Quantification of the root span is provided in Supporting Information Fig. S1. Each line was tested in at least three independent experiments with a randomized order of growth sectors per mutant.

Figure S3. Quantification of root span of seedlings grown on minimal medium supplemented with various salts. Seedlings of the genotypes indicated were grown on the minimal medium supplemented with various concentrations of (a) $SrCl_2$, (b) $MgSO_4$ and (c) $MgCl_2$. At least 15 seedlings were measured per genotype. Seedlings of each genotype were randomized and distributed on at least three plates. Data points indicate the mean ± SD from one representative experiment. The experiment was repeated independently three times, yielding similar results.

Figure S4. Characteristic phenotypes of *tua mlo* double mutants grown on minimal medium. When root curling directions were scored, images were taken for each characteristic phenotype observed: (a) single coil, anti-clockwise – mostly observed in *mlo4*-4 *tua4*^{M268I} and *mlo4*-3 *or mlo4*-4. (b) Secondary loops, anticlockwise – mostly observed in *mlo4*-3 *or mlo4*-4. (c) Single coil, clockwise – mostly observed in *mlo4*-3 *or mlo4*-4. (d) Secondary loops, clockwise in first loop and anticlockwise in second – please note less tight loops than in (c) – here an example of *mlo11*-4. (e) Clockwise – override/rollercoaster – characteristic for *mlo4*-4 *tua4*$^{S178\Delta}$. (f) Anticlockwise – wide curl – characteristic for *mlo11*-4 *tua4*^{M268I}. (g) Wavy – characteristic for *mlo11*-4 tua4$^{S178\Delta}$. (h) Wavy with tight curl – characteristic for *mlo11* tua4$^{S178\Delta}$. Scale bar: 500 μm.

Figure S5. Shoot and hypocotyl gravitropism phenotypes of selected *rcs* mutants. Photographs show the outcome (endpoint) of shoot and hypocotyl gravitropism assays for wild-type Col-0, *mlo4*-3 and the suppressor (double) mutants *mlo4*-3 *rcs1*, *mlo4*-3 *rcs2*, *mlo4*-3 *rcs3* and *mlo4*-3 *rcs4*. Note that pictures are not to scale.

Table S1. Details of mutants used in the study and quantification of *mlo4*-like root curling.

Table S2. SSLP markers polymorphic between ecotypes Col-0 and Ws-0 used for first-pass mapping.

Table S3. Quantification of root curling patterns.

Methods S1. Plant mutants and primers used in this study.

Movie S1. Time lapse imaging of seedling development and root curling phenotypes in *mlo4*-3, *mlo4*-4, *mlo11*-4, *mlo14*-7, *mlo4*-4 *mlo11*-4 *mlo14*-7 mutants and Col-0 control plants. Seedlings were treated as described in the Material and Methods section. Imaging started at ca. 24 h after transfer from 4 °C to room temperature and was performed for 84 h with one image every hour. Pictures were taken from the bottom of the plate. Imaging was carried out at ambient conditions with continuous light provided by two fluorescent bulbs placed 50 cm away from the plate with the seedlings. Pictures were taken with ProgRes® CapturePro2.7 using a ProgRes® C7 camera (Jenoptik, Jena, Germany) accommodated with a 25 mm lens (f/0.95; Jos. Schneider Optische Werke GmbH, Germany). Images were then processed with ImageJ software (http://rsb.info.nih.gov/ij/).

Movie S2. Time lapse imaging of the root curling phenotype of a *mlo4*-4 mutant seedling at 5× magnification. Seedlings were treated as described in the Material and Methods section. Imaging started at ca. 72 h after transfer from 4 °C to room temperature and was performed for ca. 40 h with one image every 10 min in continuous light conditions (light input

from the microscope lamp and a nearby table lamp). The movie was generated with a Zeiss Axiovert 135 TV microscope and JVC KY-F75U camera using Diskus software (www.hilgers.com; Königswinter, Germany). Images were then processed with ImageJ software (http://rsb.info.nih.gov/ij/).

Movie S3. Time lapse imaging of root curling phenotype of a *mlo4*-4 mutant seedling at 10× magnification. Imaging started after completion of Supporting Information Movie S2 and was performed for ca. 4 h with one picture every 2 min in continuous light conditions (light input from the microscope lamp and a nearby table lamp). The movie was generated with a Zeiss Axiovert 135 TV microscope and JVC KY-F75U camera using Diskus software (www.hilgers.com; Königswinter, Germany). Images were then processed with ImageJ software (http://rsb.info.nih.gov/ij/).